Journal of Hydrology (2007) 339, 65–78

available at www.sciencedirect.com

ScienceDirect

journal homepage: www.elsevier.com/locate/jhydrol

Representative hydraulic conductivity of hydrogeologic units: Insights from an experimental stratigraphy

Ye Zhang [a,*], Mark Person [b], Carl W. Gable [c]

[a] Department of Geological Sciences, University of Michigan, 2534 C.C. Little Building, 1100 North University Avenue, Ann Arbor, MI 48109, USA
[b] Department of Geological Sciences, Indiana University, 1001 East Tenth Street, Bloomington, IN 47405, USA
[c] EES-6, MS T003, Los Alamos National Lab, Los Alamos, NM 87545, USA

Received 30 October 2006; received in revised form 9 March 2007; accepted 19 March 2007

KEYWORDS
Hydraulic conductivity;
Heterogeneity;
Effective conductivity;
Equivalent conductivity;
Experimental stratigraphy;
Scale effect;
Stochastic theory

Summary A critical issue facing groundwater flow models is the estimation of representative hydraulic conductivity assigned to the model units. In this study, an experiment-based, high-resolution hydraulic conductivity map offers a test case to evaluate this parameter. Various hydrogeological units are distinguished, each is of irregular shape with distinct heterogeneity pattern created by physical sedimentation. Extending a previous study which used numerical upscaling to compute equivalent conductivities for these units (at two upscaling scales) [Zhang, Y., Gable, C.W., Person, M., 2006. Equivalent hydraulic conductivity of an experimental stratigraphy — implications for basin-scale flow simulations. Water Resources Research 42, W05404. doi:10.1029/2005WR004720], this study compares them with local statistics and effective conductivities predicted by a stochastic theory. Results suggest that for a system with moderate ln$K$ variance (4.07) and low topographic slope (~1°), the arithmetic mean (K_A) provides a good estimate for the maximum principal component (K_{max}) of the equivalent conductivity. The minimum principal component (K_{min}) lies between the harmonic and geometric means: its closeness to the geometric mean is affected by heterogeneity pattern and upscaling scale. Using K_{max} (alternatively, the arithmetic mean), geometric mean, and ln(K) variance, the stochastic theory predicts a K_{min} that is consistent with the up-scaled value. Similarly, knowing K_{min}, K_{max} predicted by theory is also consistent with the up-scaled value. For most deposits (some with variance greater than 1), a low-variance version of the theory is more accurate than a high-variance version. However, the increase of topographic slope (to ~4°) and total ln$K$ variance (to 16) result in increased deviation of K_{max} from K_A. High variance also results in significantly larger anisotropy ratio, possibly due to the dominance of

* Corresponding author. Tel.: +1 734 6153055; fax: +1 734 7634690.
E-mail address: ylzhang@umich.edu (Y. Zhang).

0022-1694/$ - see front matter
doi:10.1016/j.jhydrol.2007.03.007

preferential flow. Finally, for select units, equivalent conductivity exhibits scale effect. Field scale representative elementary volume thus does not exist and upscaling the full unit is necessary to obtain the representative conductivity.

Introduction

In field to regional scale groundwater studies, hydrogeological framework models are routinely used to evaluate a variety of geological and environmental processes. In these models, based on facies mapping, sedimentary deposits are represented by distinct hydrogeologic units, e.g., sandstone, claystone, limestone. A representative saturated hydraulic conductivity is assigned to each unit to relate the mean head gradient to the average groundwater flux. The effect of within-unit stratification is represented by an anisotropy ratio, often arbitrarily assigned to each unit and is then subject to model calibration. Ideally, the representative conductivity quantifies the effect of underlying heterogeneity on bulk fluid movement under various flow conditions. However, in actual modeling, the estimation of representative conductivities for the model units remains a difficult task, as information on formation conductivity is commonly lacking.

If small-scale measurements are available (e.g., grain size analysis, borehole sampling), direct averages can be used to construct a representative conductivity: harmonic (K_H), geometric (K_G), arithmetic (K_A) means. It is well established that K_A and K_H are the representative lateral and vertical conductivities, respectively, for an infinite horizontal medium containing stratifications of uniform thickness. For other heterogeneity patterns, $[K_H, K_A]$ constitutes an analytic ''Wiener Bounds'' (Renard and de Marsily, 1997). However, natural hydrogeologic units are of irregular shapes, finite in extent, and contain stratifications that may or may not be spatially continuous. For these deposits, it is less clear how small-scale measurements relate to the representative conductivity, nor is the role of within-unit heterogeneity on such relationships clearly understood. To understand this, a complete description of heterogeneity is required, a near impossibility even with exhaustive sampling (Eggleston and Rojstaczer, 1998).

A representative conductivity can also be estimated using stochastic theories which treat the local conductivity (K) as a random space function (RSF) (*e.g.* Matheron, 1967; Matheron and de Marsily, 1980; Gelhar and Axness, 1983; Dagan, 1993). An *effective* conductivity is estimated based on the geostatistic parameters of natural log conductivity $-\ln(K)$. The effective conductivity is considered an intrinsic property of the RSF, thus independent of the boundary condition. However, theories often require a ''large'' system scale many times the $\ln(K)$ correlation; perturbation-based approaches may be sensitive to $\ln(K)$ variance. To test the theories for effective conductivity, numerous studies have been carried out, using field experiments (*e.g.* Sudicky, 1986; Hess et al., 1992), laboratory studies (*e.g.* Barth et al., 2001; Danquigny et al., 2004; Fernandez-Garcia et al., 2005), and numerical analyses (*e.g.* Ababou et al., 1989; Dykaar and Kitanidis, 1992; Sanchez-Vila et al., 1995; Naff et al., 1998; Paleologos et al., 2000; Jankovic et al., 2003). However, field experiments suffer parameter uncertainties due to data paucity or sampling biases; insights obtained from laboratory or numerical analyses are limited to artificially packed or synthetic data that satisfy specific statistical assumptions, e.g., stationarity, (multi-Gaussian) log-normality, exponential covariance. Natural deposits may not satisfy these assumptions, e.g., within-unit stratifications often exhibit long range correlation. It is not clear whether theories should work for such deposits.

In the last two decades, it is increasingly recognized that sedimentary structures dominate conductivity heterogeneity (*e.g.* Fogg, 1990; Anderson, 1997; Webb and Davis, 1998; Pickup and Hern, 2002). By combining geologic information with analysis on small-scale heterogeneity, multi-scale conductivity has been explicitly modeled (*e.g.* Jussel et al., 1994b; Webb and Anderson, 1996; Scheibe and Yabusaki, 1998; Bersezio et al., 1999). Various assumptions concerning heterogeneity are made, resulting in large uncertainties in the predicted conductivity, e.g., when facies units are modeled, within-unit conductivity is assumed uniform (Scheibe and Freyberg, 1995; Weissmann et al., 2002). Other studies use geostatistic simulations to generate within-unit heterogeneity, assuming diverse correlation functions (Jussel et al., 1994a; Bierkens, 1996; Lu et al., 2002; Zhou et al., 2003).

In this study, the recognition that multi-scale conductivity heterogeneity exists on the one hand, and the practical need to construct groundwater flow simulators which rely on hydrogeologic units and representative conductivity on the other, motivates an analysis based on a two-dimensional fully heterogeneous hydraulic conductivity map, created by scaling up an experimental stratigraphy (Fig. 1a). This stratigraphy is obtained from high-resolution imaging of deposits generated in a fluvial experiment where multiple sedimentary facies formed in response to a variety of depositional processes (*e.g.* Paola, 2000). By assuming appropriate length scales, each image pixel is scaled up to the dimensions of a representative elementary volume (REV). Based on pixel gray scale and two end-member conductivities (one for pure sand, one for pure clay), a scalar, local-scale conductivity is obtained via log-linear interpolation and defined for each REV. The $\ln(K)$ variance of the map is 4.07, reflecting the range of an unconsolidated alluvial fan. Since the conductivity map corresponds to physical stratigraphy, it exhibits multi-scale variability and may not satisfy any statistical assumptions. In light of the framework model approach, the map is divided into 14 depositional units (Fig. 1b), and alternatively, a global aquifer and aquitard (Fig. 1c). The aquitard consists of the clay-rich units of 1, 7, 13, 14; the aquifer is the sand-rich units combined.

This study is an extension of earlier studies in which details on this map can be found. For select subregions,

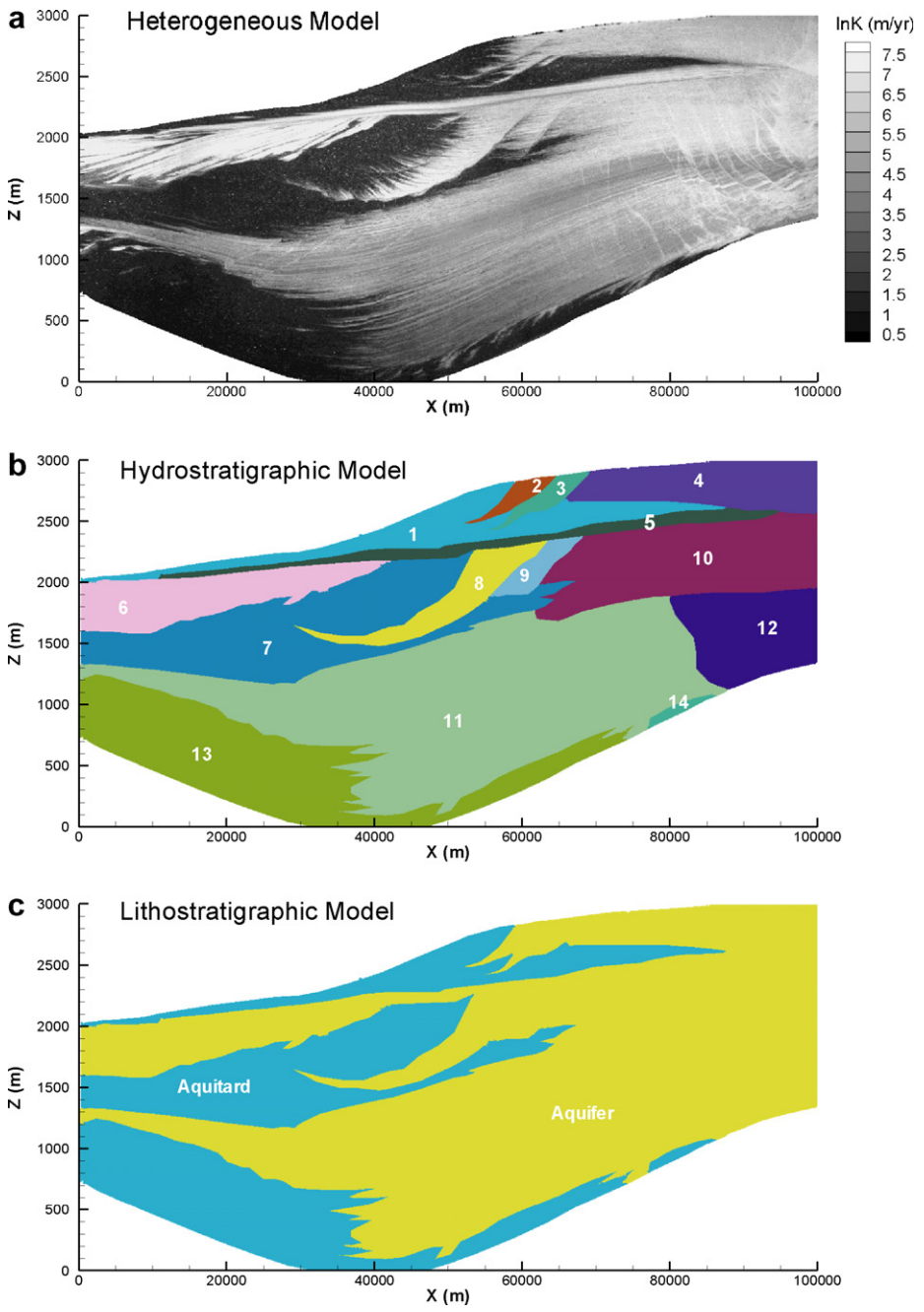

Figure 1 (a) Basin-scale ln*K* map (in m/yr); (b) a 14-unit model with the unit ID: 1—14; (c) a 2-unit model.

Zhang et al. (2005) calculated experimental ln(*K*) variograms along the principal statistical axis. Using numerical simulations, Zhang et al. (2006) computed *equivalent* or *up-scaled* conductivities for these units (Fig. 1b and c). These conductivities were found consistent with the predictions of a low-variance stochastic theory. However, the theory was not used in direct predictions. Though a high-variance version exists, its applicability was not assessed. In this study, the equivalent conductivities are compared to direct averages of within-unit conductivity, and, to an effective conductivity predicted explicitly by theory. Both a low- and high-variance version of the theory are tested. A sensitivity analysis is further conducted by alternatively increasing the topographic slope (via changing domain aspect ratio) and the total system variance (to 16.0). Results are again compared to direct averages and theory predictions. We explore the conditions of obtaining representative conductivity using statistical moments and theories, without resorting to high-resolution simulations.

Finally, conductivity ''scale effect'' is a well-known phenomenon whereby measured values change (often increase) with data support (Neuman, 1990, 1994; Doll and Schneider, 1995; Sanchez-Vila et al., 1996; Rovey, 1998;

Butler and Healey, 1998; Schulze-Makuch et al., 1999; Zlotnik et al., 2000; Hyun et al., 2002; Martinez-Landa and Carrera, 2005). Various explanations are proposed, e.g., deviation from log-normality, fractal porous media, non-stationarity, and measurement artifacts. Due to difficulties in determining the support volume, the exact mechanism behind the scale effect is not clear. However, a related concept of field scale REV (FSREV) is developed: representative conductivity of a formation is assigned a value at which smaller scale conductivity reaches a plateau. This FSREV is assumed to correspond to a statistical homogeneity which is then assumed to repeat in the formation of interest, eliminating the need for exhaustive sampling. Such an assumption underlies most of the large scale flow models. However, the existence of FSREV is never tested. In this study, the scale effect is evaluated by numerically upscaling various subregions and comparing the equivalent conductivities with both local averages and the equivalent conductivity of the full unit. We inspect (1) whether scale effect exists and what may be responsible; (2) can a FSREV be found, thus eliminating the need for full-unit upscaling?

In this study, heterogeneity and the associated statistics are fully known, eliminating parameter uncertainties encountered in field studies. Compared to laboratory analyses, the various units analyzed may or may not satisfy theory assumptions. Compared to numerical simulations which employ a stochastic framework to evaluate effective conductivity and uncertainties (i.e., many realizations of the detailed heterogeneity are created, theory prediction is compared to an ensemble average), this study employs a deterministic view, i.e., comparing theory predictions with one set of equivalent conductivities. (Alternatively, if the conductivity map is posed as one realization of a RSF, the comparison is made assuming ergodicity.) As theory is continuously being tested and refined, the next logical step is to evaluate its applicability for realistic heterogeneities. The deposit of this study presents such a test case to evaluate theory.

In the reminder of the text, the upscaling method is briefly described along with the formulations of the stochastic theory. Results pertaining to Fig. 1a (basin scale, moderate variance) are presented, followed by a sensitivity analysis. The implications for parameter estimation using theory are discussed. A section on conductivity scale effect is then presented. We end with indicating directions for future research.

Mathematical formulations

Conductivity upscaling

Upscaling for the irregular hydrogeologic units is conducted using global flow simulations. The conductivity map is discretized down to the scale of each pixel. A high density finite element grid is created with 424,217 nodes and 845,208 elements. A series of steady state, incompressible flow experiments is conducted in the heterogenous model by varying the boundary condition along the domain periphery. For each unit, an equivalent conductivity is obtained by incorporating results from all experiments:

$$\text{B.C.1}: \begin{Bmatrix} \langle q_x\rangle_1 \\ \langle q_z\rangle_1 \end{Bmatrix} = -\begin{bmatrix} K_{xx} & K_{xz} \\ K_{zx} & K_{zz} \end{bmatrix} \begin{Bmatrix} \langle \partial h/\partial x\rangle_1 \\ \langle \partial h/\partial z\rangle_1 \end{Bmatrix}$$

$$\cdots$$

$$\text{B.C.}m: \begin{Bmatrix} \langle q_x\rangle_m \\ \langle q_z\rangle_m \end{Bmatrix} = -\begin{bmatrix} K_{xx} & K_{xz} \\ K_{zx} & K_{zz} \end{bmatrix} \begin{Bmatrix} \langle \partial h/\partial x\rangle_m \\ \langle \partial h/\partial z\rangle_m \end{Bmatrix}$$

$$\begin{bmatrix} \langle \partial h/\partial x\rangle_1 & \langle \partial h/\partial z\rangle_1 & 0 & 0 \\ 0 & 0 & \langle \partial h/\partial x\rangle_1 & \langle \partial h/\partial z\rangle_1 \\ \cdots & \cdots & \cdots & \cdots \\ \langle \partial h/\partial x\rangle_m & \langle \partial h/\partial z\rangle_m & 0 & 0 \\ 0 & 0 & \langle \partial h/\partial x\rangle_m & \langle \partial h/\partial z\rangle_m \end{bmatrix} \begin{Bmatrix} K_{xx} \\ K_{xz} \\ K_{zx} \\ K_{zz} \end{Bmatrix} = -\begin{Bmatrix} \langle q_x\rangle_1 \\ \langle q_z\rangle_1 \\ \cdots \\ \langle q_x\rangle_m \\ \langle q_z\rangle_m \end{Bmatrix} \quad (1)$$

where $\langle\rangle$ represents spatial averaging; q_x, q_z are components of the Darcy flux; K_{xx}, K_{xz}, K_{zz} are components of the equivalent conductivity (symmetry is imposed, i.e., $K_{xz} = K_{zx}$); h is hydraulic head; m is the number of flow experiments ($m \geqslant 2$). In this study, $m = 4$. The relevant boundary conditions are: (1) vertical mean flow: top and bottom boundaries are specified head; no flow for the sides; (2) lateral mean flow: top and bottom are no flow; specified head for the sides; (3) topography-driven flow: specified head for the top boundary; no flow for all others; (4) same as (3) except a set of fluid source/sink is imposed with a rate of 10,000 m/yr. The equivalent conductivities are obtained via least square solution. More details on the upscaling method including grid generation can be found in Zhang et al. (2006).

Stochastic theory

Many theories have been developed to estimate effective conductivity for which a well-known result for anisotropic media is evaluated (Zhang, 2002, p. 143, (3.155)):

$$K_{ii}^{\text{ef}} = K_{\text{G}}\left[1 + \sigma_f^2(0.5 - F_i)\right]$$
$$F_i = \frac{1}{\sigma_f^2}\int \frac{k_i^2}{k^2} S_f(\mathbf{k})d\mathbf{k} \quad (2)$$

where K_{ii}^{ef} are components of an effective conductivity along the principal statistical axes; σ_f^2 is $\ln K$ variance; $\mathbf{k} = (k_1, \ldots, k_d)^{\text{T}}$ is the wave number vector; d is the number of space dimensions; S_f is the spectral density of $\ln(K)$, defined as the Fourier transform of the $\ln(K)$ covariance function. Eq. (2) results from first-order approximation and is valid for stationary media with small σ_f^2. Based on the *Landau-Lifshitz* conjecture (which treats the two terms within the brackets as part of a series expansion of an exponential function), Eq. (2) is generalized to higher variance ($\sigma_f^2 > 1$) (Gelhar and Axness, 1983):

$$K_{ii}^{\text{ef}} = K_{\text{G}} \exp[\sigma_f^2(0.5 - F_i)] \quad (3)$$

For two-dimensional problems, simple relations of F_i are obtained:

$$F_1 = \frac{e}{1+e}; \quad F_2 = \frac{1}{1+e} \tag{4}$$

where $e = \lambda_2/\lambda_1$ ($0 < e \leqslant 1$) is statistical anisotropy ratio, λ_2 and λ_1 are ln(K) integral scales along the minor and major statistical axes, respectively. Note that a three-dimensional version of the theory was tested in a laboratory aquifer (Fernandez-Garcia et al., 2005). Results from both tank experiments and Monte Carlo simulations suggest that for the prescribed heterogeneity (stationary with exponential anisotropic covariance), Eq. (2) is more accurate than Eq. (3), even for deposits with $\sigma_f^2 > 1$. Specifically, Eq. (3) overestimates the maximum principal component of the effective conductivity.

Results

For the 16 hydrogeologic units (14 depositional units; aquifer; aquitard), the equivalent conductivities are diagonally dominant full tensors: $K_{max} \sim K_{xx}$, $K_{min} \sim K_{zz}$ (K_{max}, K_{min} are the principal components), reflecting the near horizontal stratigraphic dip (Table 1). In this section, both principal components are compared to local statistics and theory predictions. A sensitivity analysis is conducted by changing the domain aspect ratio and total variance. To evaluate scale effect, conductivity is computed for increasing data support.

Equivalent conductivity versus direct averages

For each unit, the mean and variance of ln(K) and the local statistics — K_H, K_G, K_A — are computed (Fig. 2a and b). K_{max} and K_{min} are compared to the Wiener Bounds (Fig. 2c). The anisotropy ratio (K_{max}/K_{min}) is also plotted (Fig. 2d). Results indicate:

(1) Mean conductivity of the various units appears bimodal, reflecting the global division of sand-rich and clay-rich units. ln(K) variance ranges from 0.31 (unit 4) to 1.85 (unit 6), comparable to many natural aquifers (Hoeksema and Kitanidis, 1985; Anderson, 1997).

(2) For all units, the principal components lie within the Wiener Bounds (derived for infinite media), suggesting that an effective conductivity has emerged, its value determined only by local averages. This is consistent with the earlier observation that the equivalent conductivity is not sensitive to boundary condition (Zhang et al., 2006). This is because the upscaling domain (i.e., a hydrogeologic unit) is generally large compared to ln$K$ integral scales (Renard and de Marsily, 1997). Note that such will not be the case when the domain is small, as often in block upscaling (Bierkens and Weerts, 1994). However, the goal of this study is not to evaluate the traditional upscaling issues, i.e., developing coarse-grid solutions for fine-grid problems and estimating the relevant coarse-grid parameters. Rather, our goal is to find representative conductivities for groundwater flow models. The lithofacies-based upscaling approach ensures that the comparison between equivalent conductivity with theory prediction of an effective conductivity is appropriate.

(3) K_{min} lies between the harmonic and geometric means: K_G is a good estimate for the weakly stratified or nearly homogenous deposits (units 4, 10, 1, 7, 13, 14); K_H is a good estimate for the more stratified deposits (unit 6). For the further up-scaled aquifer and aquitard, $K_{min} \sim K_G$: these units behave as weakly stratified, reflecting their partial continuity at the regional scale. Clearly, both heterogeneity and scale impact the upscaling characteristics.

(4) The anisotropy ratio is positively correlated to deposit variability (Fig. 3b and d): higher anisotropy is observed for higher variance. An exception is the aquifer unit which exhibits statistical heterogeneity (i.e., multiple depositional environments).

Table 1 Equivalent hydraulic conductivity (m/yr), its principal components (K_{max}, K_{min}), and the anisotropy ratio (K_{max}/K_{min})

Unit ID	Depo. Environ.	E[ln(K)]	Var[ln(K)]	K_{xx}	K_{zz}	K_{xz}	K_{max}	K_{min}	K_{max}/K_{min}
1	Deepwater	2.10	0.73	17.18	7.01	−0.25	17.18	7.01	2.45
2	Shoreline	4.73	1.48	188.96	61.36	−9.73	189.70	60.62	3.13
3	Shoreline	5.34	1.15	294.35	104.04	−6.90	294.60	103.79	2.84
4	Fluvial	5.68	0.31	330.53	256.31	1.82	330.58	256.27	1.29
5	Fluvial	5.98	0.91	554.56	224.41	−6.38	554.68	224.28	2.47
6	Turbidite	6.26	1.85	871.00	151.54	10.21	871.14	151.40	5.75
7	Deepwater	2.07	0.83	19.16	7.17	0.53	19.18	7.15	2.68
8	Shoreline	6.00	1.25	583.76	211.36	28.33	585.91	209.21	2.80
9	Shoreline	5.44	1.13	321.95	120.82	−5.15	322.08	120.69	2.67
10	Fluvial	6.29	0.37	591.62	536.97	3.92	591.90	536.69	1.10
11	Fluvial/floodplain	4.53	1.10	140.41	69.51	1.16	140.43	69.49	2.02
12	Fluvial/floodplain	5.68	0.62	388.44	213.41	0.08	388.44	213.41	1.82
13	Deepwater	1.32	0.41	5.53	3.69	0.01	5.53	3.69	1.50
14	Deepwater	2.02	0.59	11.66	6.49	0.15	11.66	6.48	1.80
—	Aquitard	1.76	0.77	13.28	5.41	−0.03	13.28	5.41	2.46
—	Aquifer	5.29	1.54	324.61	198.49	2.09	324.65	198.46	1.64

The mean and variance of ln(K) are also listed, along with the depositional environment of each unit.

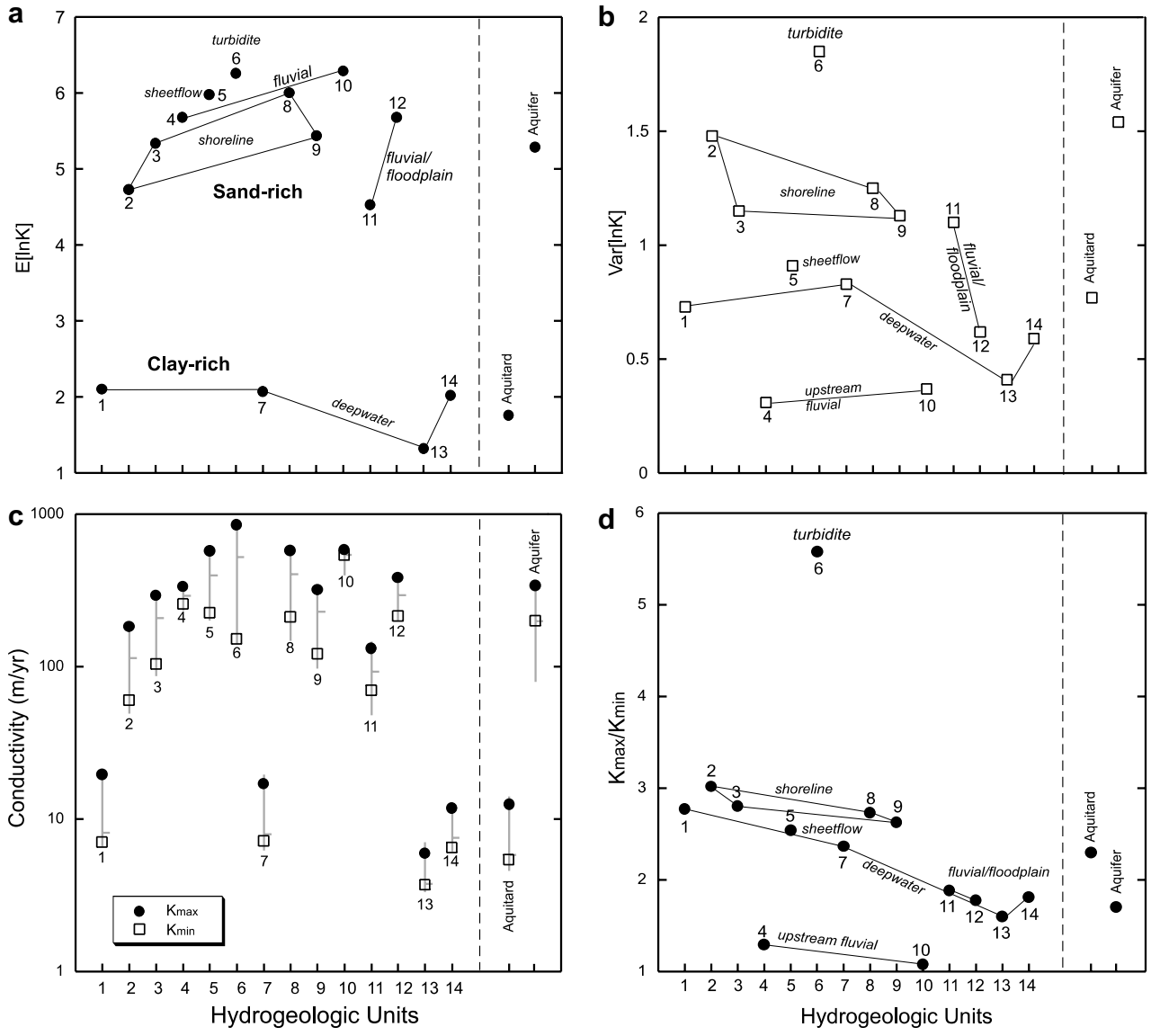

Figure 2 Statistics of the 14 depositional units and the aquifer and aquitard: (a) mean ln(K), (b) ln(K) variance, (c) equivalent conductivity principal components (K_{max},K_{min}) plotted against direct averages: [K_H,K_A] defines a gray line with K_G indicated as a cross-bar. The anisotropy ratio (K_{max}/K_{min}) (d). In (a), (b), (d), data from similar depositional environment are connected by lines.

(5) The equivalent conductivity is not additive, e.g., the principal components of the aquifer and aquitard deviate from those obtained by direct averaging the constituent units, using either arithmetic mean or weighted (by area) arithmetic mean.

Besides [K_H,K_A], more restrictive bounds are available. For example, for a lognormal distribution, Dagan (1989) obtained bounds for the effective conductivity principal components: $\exp(-\sigma_f^2/2) \leqslant K_{min}/K_G \leqslant K_{max}/K_G \leqslant \exp(\sigma_f^2/2)$. Various units in Fig. 2 are reorganized by depositional environment for which the equivalent conductivity components are plotted against these bounds (Fig. 3). Compared to the sand-rich units (principal components fall within or near the bounds), the clay-rich units has K_{max}/K_G significantly above it. These units are non-Gaussian: their ln$K$ distributions are characterized with large skewness and kurtosis. Though unit 12 contains growth ''faults'', its principal components fall neatly at the bounds. Its univariate statistics fall close to a normal distribution.

Finally, K_{max} falls close to K_A for all units and at both upscaling scales (Fig. 4). A best-fit line gives: $K_A = 1.01K_{max} + 3.03$, $R^2 = 0.998$ (not shown). This result is particularly interesting since it is observed for the stratified (units 2, 3, 6, 8, 9, 11, 12), non-stratified (units 4, 1, 7, 13, 14), weakly stratified (unit 10), and the non-stationary aquifer. In lab experiments conducted on artificially packed sands (Danquigny et al., 2004), a lateral equivalent conductivity was found equal to the arithmetic mean when the deposits were packed with emulated channels; it was between the geometric and arithmetic means when the deposits were random but of exponential covariance. Thus, if the experimental stratigraphy is considered a plausible representation of natural heterogeneity, the idealized structure

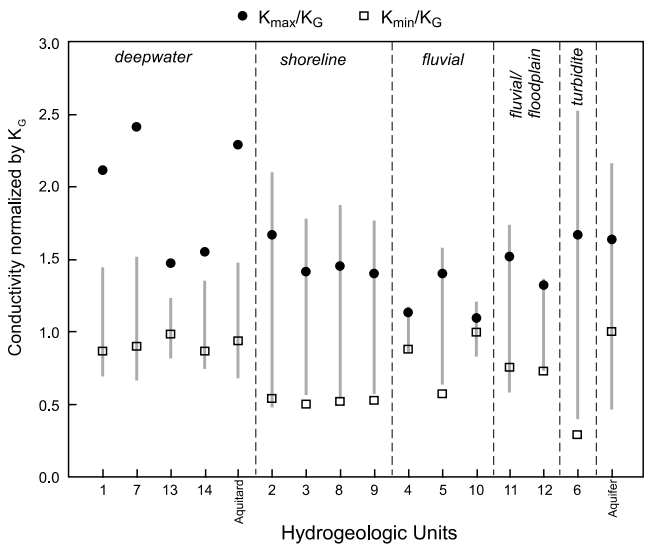

Figure 3 Equivalent conductivity principal components normalized by K_G, compared to Dagan (1989)'s bounds (vertical gray line). Units created in similar depositional environment are grouped.

(upon which most theories are based) may be rare in nature, especially in fluvial systems. However, theories may still prove robust for certain deposits and under certain conditions (next).

Equivalent conductivity versus theory prediction

For the ln(K) map (Fig. 1a), a previous geostatistical analysis indicates that the principal statistical axes are aligned close to the global coordinate axes (Zhang et al., 2005). For all units, the equivalent conductivity is diagonally dominant. Thus, comparison can be made between K_{11} and K_{max}, K_{22} and K_{min}. For each unit, K_{max} and K_{min} can be estimated with Eq. (2) or (3) using K_G, σ_f^2, and e. To ensure that additional uncertainties are not introduced during variogram modeling, we estimate one component assuming the other is known. For example, given K_{max} obtained from upscaling, an apparent e can be determined for $i = 1$. For $i = 2$, theory is used to compute an effective minimum component: K_{min}^{ef}, which is compared to the equivalent K_{min}. A relative prediction error is defined: $\text{Err}\ (\%) = (K_{min}^{ef} - K_{min})/K_{min} \times 100\%$.

Using Eq. (2), K_{min}^{ef} is estimated and compared to the equivalent K_{min} (Fig. 5a). For all units, positive correlation is apparent (the non-stationary aquifer is an exception). Despite moderate variance, the largest relative error occurs for the clay-rich units (Fig. 6a). For the rest of the sand-rich units, the error magnitude (|Err|) increases with increasing variance (not shown), as expected. Using Eq. (3), K_{min}^{ef} is also estimated (Fig. 5b). Though positive correlation with the equivalent K_{min} still exists, larger scatter is observed. The error characteristics are also different: with Eq. (2), Err ranges from -160% to 20%; with Eq. (3), Err ranges from -60% to 120% (Fig. 6a). Eq. (3) thus estimates higher value of K_{min}^{ef} than Eq. (2).

However, does Eq. (3) consistently overestimate K_{min} relative to Eq. (2)? The Err cross-plot suggests (Fig. 6a): (1) for unit 4 $(\sigma_f^2 = 0.31)$, both equations are very accurate in predicting K_{min}; (2) for unit 10 $(\sigma_f^2 = 0.37)$, both equations introduce the same deviations; (3) for all other units $(\sigma_f^2 > 0.37)$, Eq. (3) estimates higher value of K_{min}^{ef} than Eq. (2). Note that for statistically isotropic media, a cutoff variance of 4 is found for the exponential conjecture (Neuman and Di Federico, 2003). For anisotropic media, it is speculated that such cutoff should exist at smaller variance. It is the case in K_{min} estimation: 0.37 is an apparent cutoff, i.e., only when variance is significantly greater does Eq. (3) deviate from (estimate higher values than) Eq. (2). For units 5, 8, 9, 3, 6, however, both equations overestimate the equivalent conductivity (see shaded region). These units generally have the highest variances (Fig. 2b).

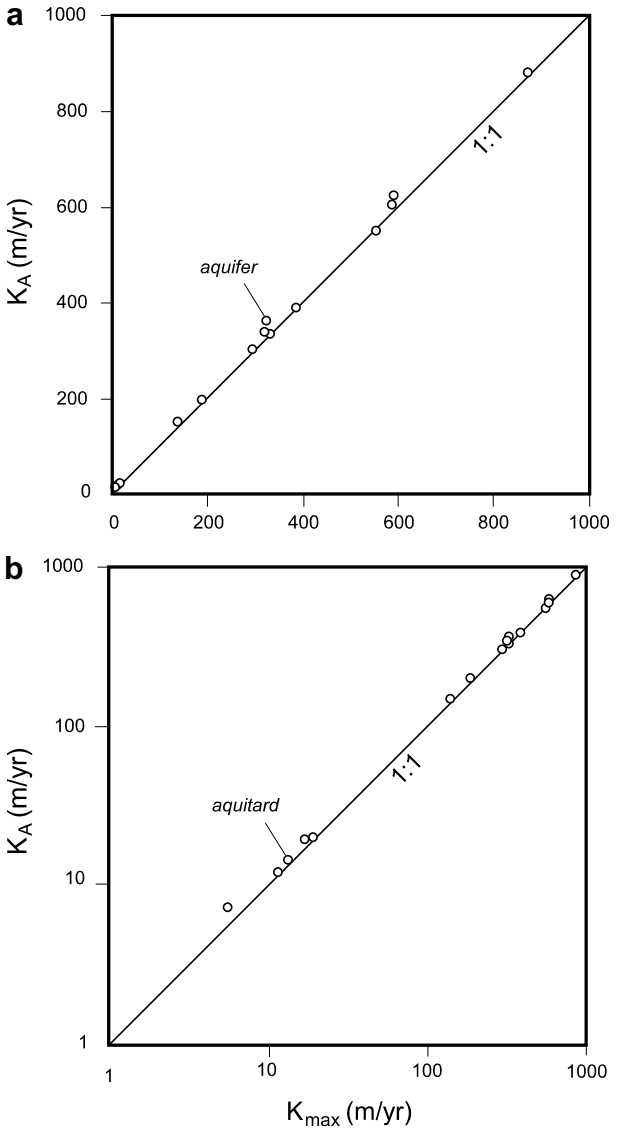

Figure 4 K_{max} of the equivalent conductivity against K_A for all 16 units, in linear (a) and log–log space (b).

In practice, upscaling based on fully known heterogeneity is rarely possible, but sampling programs may estimate a mean conductivity. Since $K_{max} \sim K_A$, the above analysis is repeated by replacing K_{max} with K_A. Prior observations exactly hold, e.g., using Eq. (3), the best-fit line to Fig. 5b is only slightly different: $y = 0.94x + 20.78$, $R^2 = 0.85$. In this

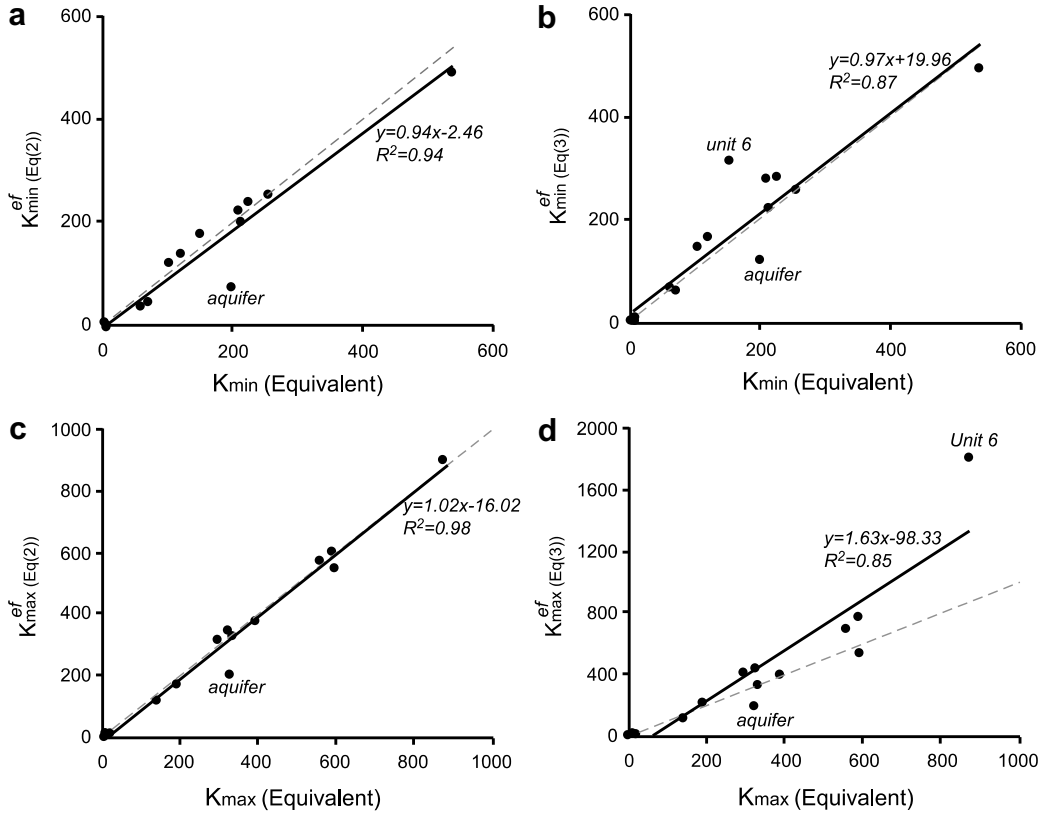

Figure 5 (a) Given K_{max}, K^{ef}_{min} estimated with Eq. (2) compared to the equivalent K_{min}. A best-fit line is shown with the fitting coefficient. Dashed line is perfect correlation. (b) K^{ef}_{min} estimated with Eq. (3) compared to the equivalent K_{min}. K^{ef}_{max} estimated with both equations are shown in (c) and (d), respectively, against the equivalent K_{max}. All conductivities are in m/yr.

case, local statistics — K_A, K_G, σ_f^2 — can be used to estimate a representative conductivity, *without* conducting flow simulations. This is a significant observation considering the field practice of using an arbitrary anisotropy ratio to obtain a vertical conductivity before model calibration. It points to the potential of using theory to predict conductivity for realistic heterogeneities, rather than for synthetic data specifically designed to satisfy theory assumptions. However, in this study, exact local statistics can be obtained from the fully known heterogeneity. Successful application of such an approach to field situations will depend on obtaining representative statistics given limited sampling.

Finally, given K_{min}, K^{ef}_{max} can also be estimated using both equations. Again, Eq. (2) is more accurate than Eq. (3) (Fig. 5c and d). For the high-variance units, Eq. (3) predicts higher values than Eq. (2) (Fig. 6b). (As in K_{min} prediction, for the low-variance units, both equations are equally accurate.) These observations apply to units with $\sigma_f^2 > 1$, consistent with the findings of Fernandez-Garcia et al. (2005). Compared to the equivalent conductivity, Eq. (3) can significantly overestimate both principal components for the high-variance deposits. In this case, the higher-order terms introduced by the exponential conjecture become important. Note that a perturbation analysis based on second-order approximation (up to σ_f^4) indicates that effective conductivity may depend on the shape of the correlation function (Indelman and Abramovich, 1994). Future work may evaluate this formulation, again by comparing theory predictions to the equivalent conductivities.

Sensitivity analysis

Aspect ratio (field scale)

The image is rescaled to 100 m long and on average 8 m thick. Compared to the previous length-to-depth ratio of 50, the new ratio is 12.5. The average topographic slope is 4%, large compared to most site-specific systems (Belitz and Bredehoeft, 1990). Additional experiments are conducted in the heterogeneous model using two global boundary conditions: specified head for the top and bottom boundaries and no flow for the sides; a lateral head gradient with no flow for the top/bottom boundaries. Because of the greater bedding angle, on average, K_{xx} is 6.5% smaller than those of the basin scale, K_{zz} is 5.4% larger, and the magnitude of K_{xz} is 4.4 times larger, as expected. For most units, however, the equivalent conductivity is still diagonally dominant. The principal components and the anisotropy ratio are also computed. When comparing K_{max} with K_A (Fig. 7a and b), larger scatters are observed compared to Fig. 4. A best-fit line gives: $K_A = 1.04K_{max} + 5.12$, $R^2 = 0.99$ (not shown). With the exception of unit 5, K_{max} is 0.7—15.4% smaller than K_A for the sand-rich units and 4.0—28.0% smaller than K_A for the clay-rich units. K_{max} of unit 5 is higher than K_A by 6.4%, falling outside the Wiener Bounds. When comparing the anisotropy ratio with that of the basin-scale problem, with the exception of unit 5, a 0.8—27.9% reduction is observed (Fig. 7c), consistent with the new domain aspect ratio. Moreover, comparing the principal components with theory predictions indicates similar error ranges

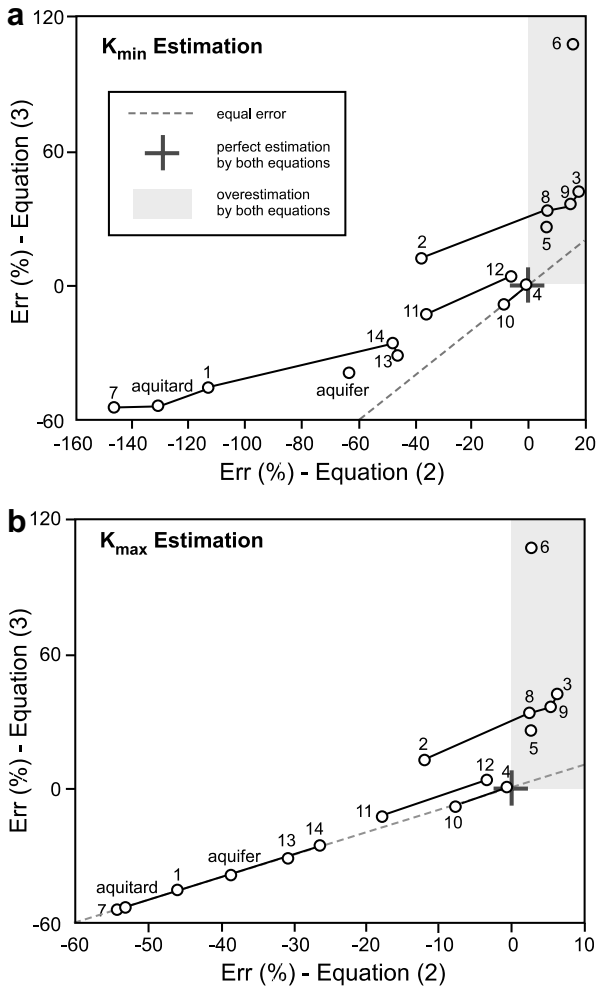

Figure 6 The relative error cross-plot using the stochastic theory: (a) K_{min} estimation given K_{max}. The effective K_{min}^{ef} is predicted by both equations; its values compared to the single, equivalent K_{min}. For each equation, a relative error is computed. (b) K_{max} estimation given K_{min}.

and characteristic distributions as those of the basin scale (not shown). Such insensitivity suggests that for the new geometry, theory is again applicable, i.e., for the low-variance sand-rich deposits.

High variance

In the previous analyses (basin scale versus field scale), the system ln(K) variance is fixed. Though such variance equals that of an alluvial fan (Zhang et al., 2005), the variance of the individual hydrogeologic units is generally modest (<2) (Fig. 2b). This reflects the end-member conductivities selected based on sand/clay mixtures. However, for more consolidated rocks, the total variance is expected to be larger. For the *same* basin geometry, additional simulations are conducted (using the same boundary conditions as above) based on a total variance of 16. This value reflects the upper limit of variability for sedimentary rocks (Gelhar, 1993). The variance increase is accomplished by rescaling the elemental ln$K$ while keeping the same arithmetic mean (Fig. 8). Compared to the previous analyses (dashed line), the end-member conductivities now reflect those of shale (0.02 m/yr) and unconsolidated sand (6×10^4 m/yr).

Results indicate that both principal components fall within the Wiener Bounds (Fig. 9a): K_{max} is 0.3—49.0% smaller than K_A for the sand-rich units and 7.0—93.5% smaller than K_A for the clay-rich units. K_{min} again falls between the harmonic and geometric means. The overall bimodal characteristics are similar to those of the low-variance system, but important differences exist. In particular, the anisotropy ratio (K_{max}/K_{min}) has significantly increased (Fig. 9b). Since high variance accentuates the effect of preferential flow, high-K deposits will dominate the global flux within a unit. Qualitatively, this is consistent with the results obtained using a network percolation model when equivalent permeability is evaluated for channel sand embedded in clay matrix, at low to moderate tortuosity (Ronayne and Gorelick, 2006). For comparison, the anisotropy ratio of the field scale problem is also plotted. Clearly, compared to the domain aspect ratio, variance exerts a dominant control on K_{max}/K_{min}.

Comparing the principal components with theory predictions reveals large relative errors, reaching up to 8000% for deposits with high-variance or non-Gaussian characteristics (not shown). It is considerably smaller for deposits of relatively low variance (e.g., 0.1—28.2% for units 4 and 10, respectively). In general, however, theory is no longer appropriate for direct prediction, i.e., assuming one or the other component is known. Interestingly, comparing the anisotropy ratio with that predicted by the high-variance theory (Eq. (3)) again reveals positive correlation between variance and anisotropy ratio (Fig. 9c). Notice the similarity with the earlier comparison for the low-variance system using the low-variance theory (Fig. 7c). Clearly, such correlation is independent of domain aspect ratio, variance scaling, and theory assumptions.

Scale effect

Conductivity scale effect is an important issue in deciding whether a hydrogeologic unit can be partially sampled via a representative region. In this study, for select units exhibiting diverse heterogeneities (i.e., the basin-scale problem in Fig. 1), equivalent conductivity is computed for subregions of increasing area (data support) and its value compared to that of the full unit. The upscaling is conducted using a local approach by imposing periodic boundary condition (Durlofsky, 1991). A five-point block-centered finite difference code is developed and validated by solving for problems with known analytic solutions (Zhang, 2005). For the subregions, 37 high-resolution grids are built where each pixel is again represented by a numerical grid cell (the number of cells ranges from 625 to 39,431). Since the flow matrix is non-symmetric, a general iterative matrix solver (DGMRES) is used with a diagonal scaling pre-conditioner, following the solution procedure of Durlofsky (1991). For each subregion, local statistics (K_H, K_G, K_A) are also computed. The aim of the analysis, however, is not to evaluate whether the equivalent conductivity converges to effective conductivity (which requires random trials at different locations and estimating an ensemble average). Rather,

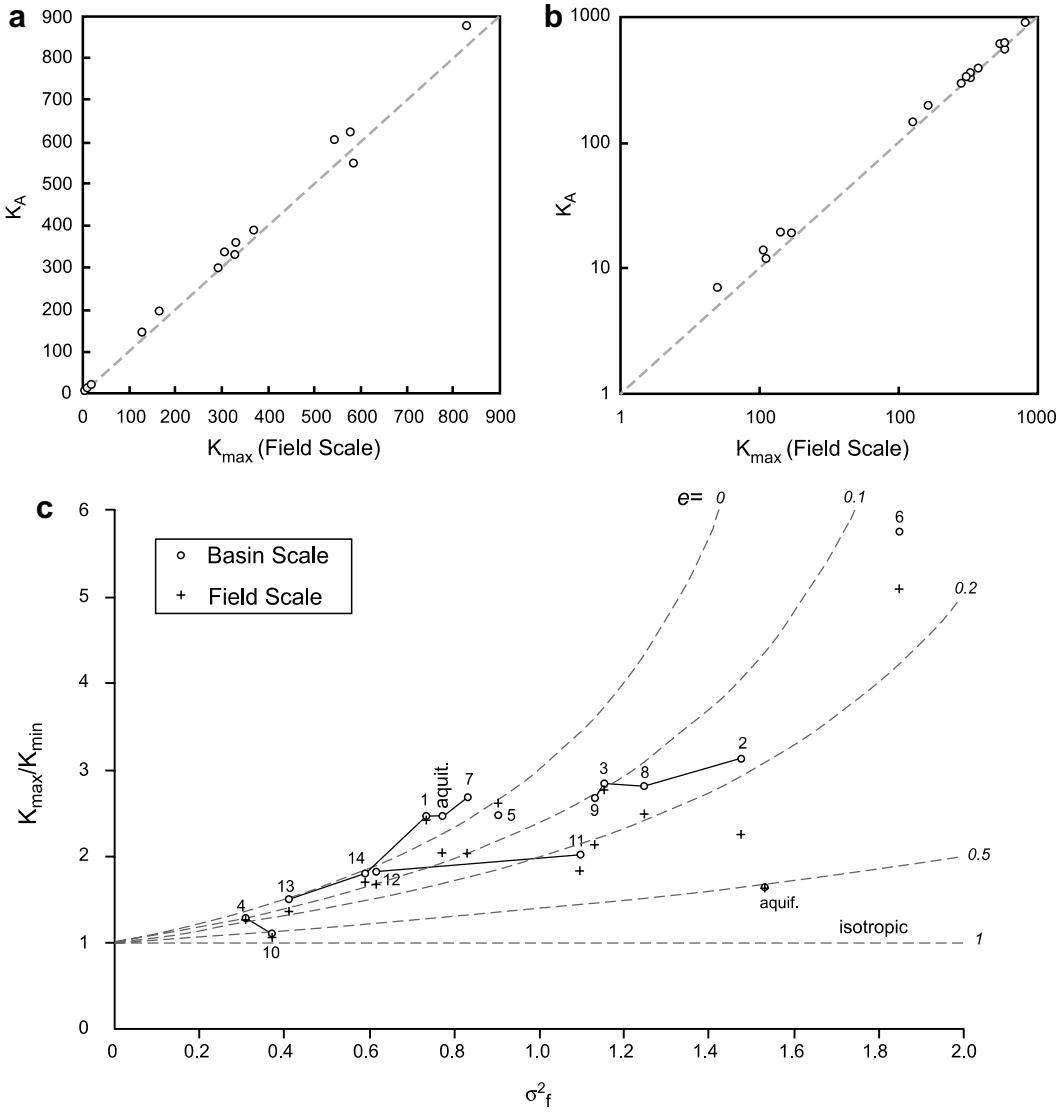

Figure 7 (a) Field scale K_{max} plotted against K_A, in linear (a) and log—log space (b). (c) Anisotropy ratio versus variance. Both basin-scale and field-scale results are shown. The low-variance theory prediction is plotted for different e (dashed lines).

the support is increasing from a fixed location to evaluate the effect of increasing aquifer volume such as encountered in field tests with different measuring devices.

Results suggest that the equivalent conductivity can increase, decrease, or fluctuate with support (Fig. 10). Such variation is controlled by the change in mean conductivity (i.e., the polynomial function fitted to K_G). Compared to the underlying heterogeneity, stratified deposits generally observe: $K_{max} \sim K_A$, $K_{min} \sim K_H$ at all supports; non-stratified deposits are clustered around K_G, as expected. Though asymptotic behavior is observed for unit 12, most do not exhibit such behavior: there are often irregular shifts in mean conductivity, likely due to global non-stationarity as a result of changing sediment transport mode. For example, in unit 7, little scale effect is apparent until the full unit scale. This is because mean conductivity does not vary until the full unit which incorporates more aquifer materials. Since non-stationarity persists at all length scales (i.e., changing mean K with support), for the units analyzed, a representative conductivity is only reached at the full unit scale (FSREV thus does not exist). Clearly, unless evidence points to extreme homogeneity (Schulze-Makuch and Cherkauer, 1998; Schulze-Makuch et al., 1999), upscaling based on subsampling will not likely be representative.

It is of interest to note that the experimental stratigraphy, though created under simplified conditions, displays non-stationary features nevertheless. In nature, other complexities can also come into play, e.g., sediment compaction and diagenesis. Though the above insights are obtained for a two-dimensional system, similar depositional variability is expected to exist in three dimensions. It is not surprising that scale effect is prevalent in natural heterogeneous deposits. Geological insights on sediment source, transport regime, and post-depositional processes will be useful in identifying trends. For example, in regional aqui-

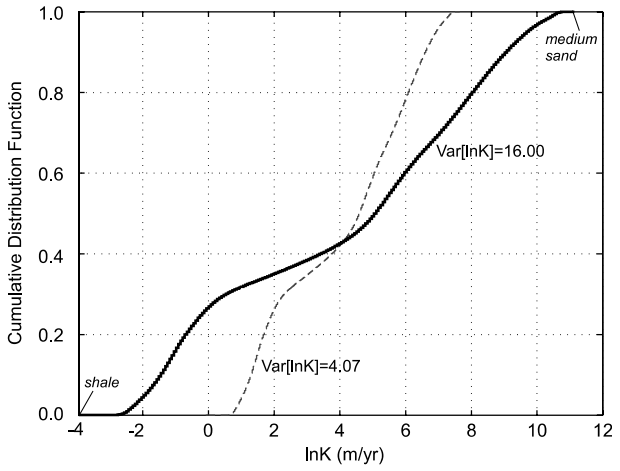

Figure 8 Cumulative distribution of the full map: small variance (dashed) versus large variance (bold).

fers in intermountain or alluvial basins, sediment grain size typically decreases from uplifted source areas toward basin interior. In such deposits, as field tests incorporate ever larger aquifer volumes, the mean conductivity changes, so does the equivalent conductivity.

Conclusions and future work

In constructing groundwater flow models, limited knowledge on the subsurface environment results in large uncertainties in the representative conductivities assigned to the model units. Due to scale effect, conductivities measured in the field are often not representative of the full unit; those obtained from model calibration are non-unique, which impacts our confidence in model predictions. In this study, a high-resolution heterogeneous hydraulic conductivity map offers a unique opportunity to evaluate our ability to estimate this parameter. Various hydrogeological units are distinguished, each is of irregular shape with distinct heterogeneity pattern corresponding to physical sedimentation. Extending a previous study which used numerical upscaling to compute equivalent conductivities, this study compares them with local statistics and effective conductivities predicted by a stochastic theory. Additional upscaling is also conducted to evaluate scale effect.

Results suggest that in a system with moderate variance and low topographic slope, the arithmetic mean (K_A) is a good estimate for the maximum principal component (K_{max}) of the equivalent conductivity. The minimum principal component (K_{min}) lies between the harmonic and geometric means: its closeness to the geometric mean is affected by heterogeneity pattern and upscaling scale. Using K_{max}

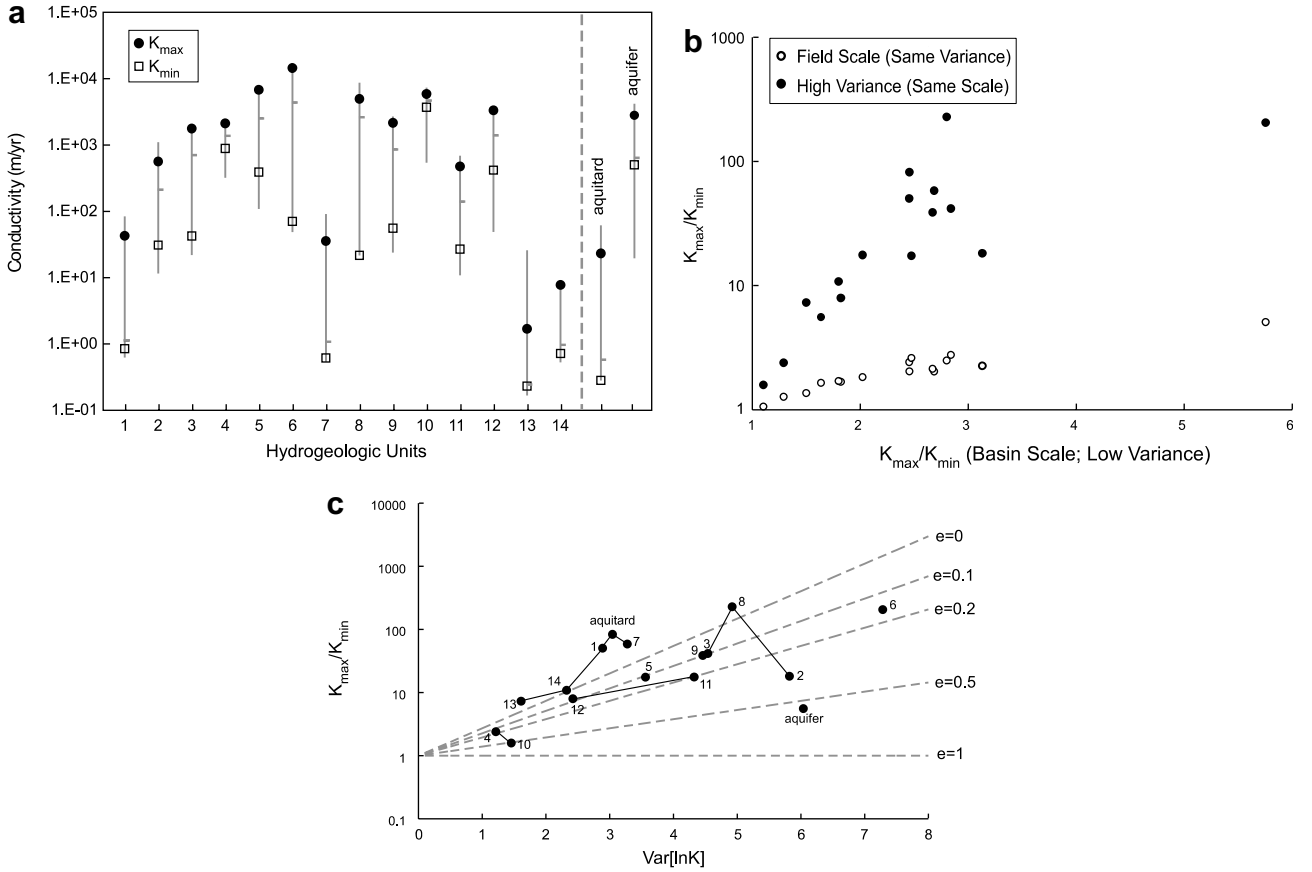

Figure 9 (a) Equivalent conductivity principal components plotted against the Wiener Bounds (K_G is indicated as a cross-bar). (b) Anisotropy ratio cross-plot: basin scale versus field scale; low-variance versus high variance. (c) Anisotropy ratio of the high-variance system against theory prediction for different e (dashed lines).

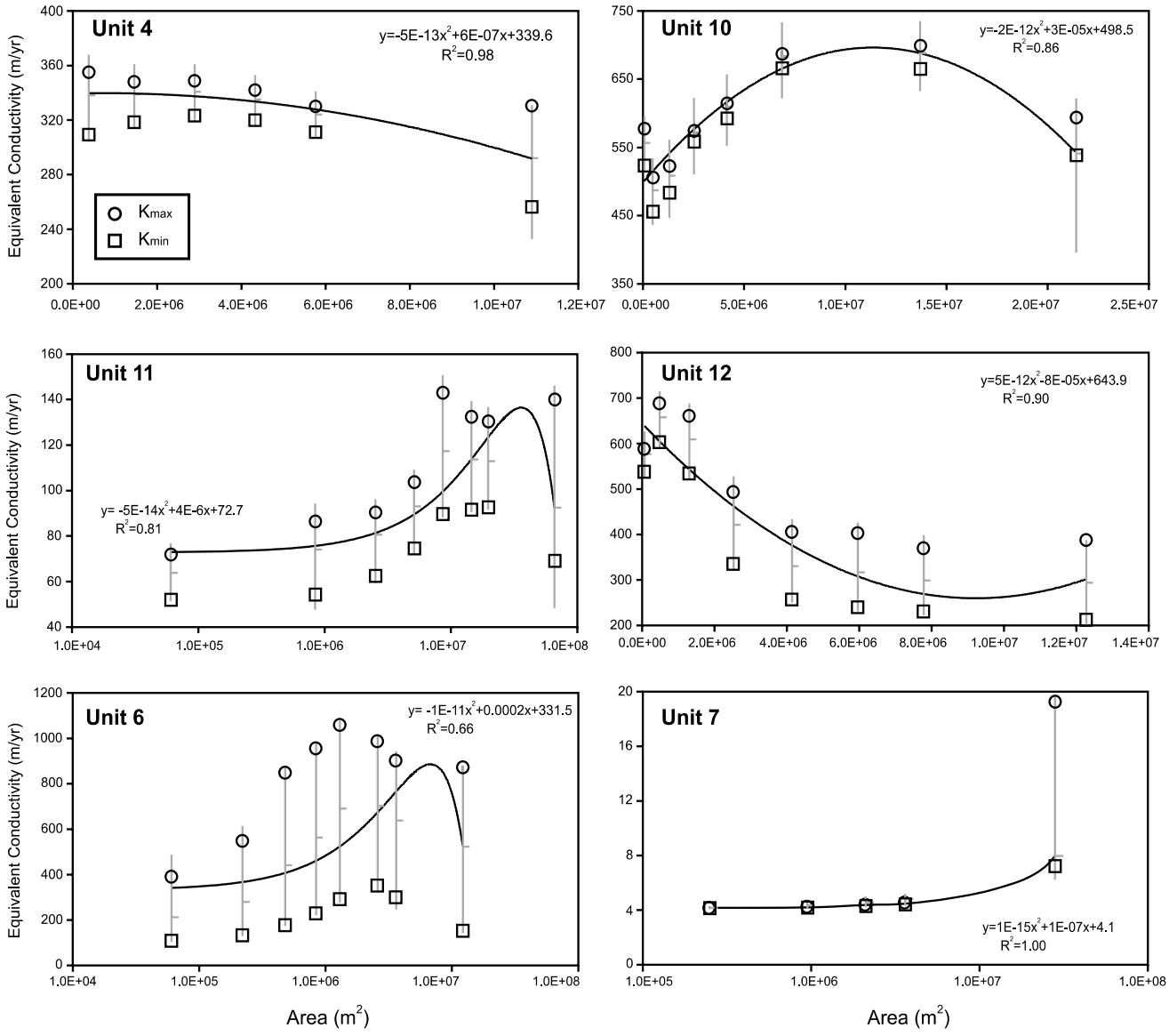

Figure 10 Equivalent conductivity principal components against data support for select units and their subregions. At each support, the local statistics are also plotted: $[K_H, K_A]$ a gray line; K_G a cross-bar. A polynomial function is fitted to K_G.

(alternatively, the arithmetic mean), geometric mean, and ln(K) variance, the stochastic theory predicts a K_{min} that is consistent with the up-scaled value, pointing to the potential of using theory to predict the anisotropy ratio. Similarly, knowing K_{min}, K_{max} predicted by theory is also consistent with the up-scaled value. For most deposits (some with variance greater than 1), a low-variance version of the theory is more accurate than a high-variance version, consistent with the findings of Fernandez-Garcia et al. (2005). Specifically, for deposits with high variance, the high-variance theory can significantly overestimate both principal components. (For low-variance deposits, both versions are equally accurate.) However, the increase of topographic slope and total variance results in increased deviation of K_{max} from K_A. High variance also results in significantly larger anisotropy ratio, possibly due to the dominance of preferential flow. Finally, for select units, equivalent conductivity exhibits scale effect which is controlled by global non-stationarity in mean local conductivity. Thus, field scale representative elementary volume does not exist and upscaling the full unit (based on either numerical or analytical approaches) is necessary to obtain a representative conductivity.

The above insights are strictly for two dimensions, though an upscaling analysis conducted on three-dimensional deposits (interconnected channel facies embedded in low-K deposits) also indicates a maximum equivalent conductivity equal to the arithmetic mean (Fogg et al., 2000). Note that our K_{min} lies between the harmonic and geometric means while the vertical and along-strike effective values of Fogg et al. (2000) are larger than the geometric mean. This is likely due to the connectivity effect in the third dimension which acts to elevate the effective values. By comparing the two studies, however, dimensionality appears to have little impact on the characteristics of the maximum principal component. Moreover, compared to many studies that attempt to find a block equivalent conductivity, the upscaling

domain of this study (i.e., a hydrogeologic unit) is lithofacies based. Each unit is typically much larger than the within-unit heterogeneity, thus the generally good match to theory predictions. However, such insights cannot be extended to block upscaling unless the same criterion is met. As correctly pointed out by the reviewer, our results may be specific to the heterogeneity we investigated. However, the methodology we developed is easily applicable to the study of other heterogeneities as well as three-dimensional data sets. Thus, our insights may ultimately be tested by conducting additional numerical, laboratory and field studies.

In future work, three-dimensional systems will be evaluated, as new deposits are created from processes operating at even smaller scales, e.g., point bar formation. Three-dimensional theories will be tested. Along with numerical upscaling, additional insights on scale effect may be gained. In the new experiments, different grain sizes and materials are used. Upscaling on these heterogeneities, whether it provides similar insights to those of this study, will be of significant interest. The link between sediment transport, heterogeneity formation, and upscaling characteristics will be evaluated. Finally, forward numerical and analytic approaches are used in this study to estimate the representative conductivities. Based on flow simulations in the heterogeneous model, future work may evaluate alternative, inverse methods for conductivity estimation.

Acknowledgements

We acknowledge the helpful communications with Dr. Xian-Huan Wen who provided an independent validation of the PBC code. We also acknowledge the insightful comments made by the anonymous reviewers. All computing was conducted on the IBM-SP and AVIDD-B of Indiana University. We acknowledge the assistance of Mr. David Hancock and Mr. Matt Allen from the University Information and Technology Service. This work was supported by the Institute of Geophysics and Planetary Physics, Los Alamos National Lab.

References

Ababou, R., McLaughlin, D., Gelhar, L., Tompson, A.F.B., 1989. Numerical simulation of three-dimensional saturated flow in randomly heterogeneous porous media. Transport in Porous Media 4, 549–565.

Anderson, M.P., 1997. Characterization of Geological Heterogeneity. Cambridge University Press, pp. 23–43.

Barth, G.R., Hill, M.C., Illangasekare, T.H., Rajaram, H., 2001. Predictive modeling of flow and transport in a two-dimensional intermediate-scale, heterogenous porous medium. Water Resources Research 37 (10), 2503–2512.

Belitz, K., Bredehoeft, J.D., 1990. Role of Confining Layers in Controlling Large-Scale Regional Groundwater FlowHydrogeology of Low Permeability Environment. Verlag H. Heise, Hannover, Germany, pp. 7–17.

Bersezio, R., Bini, A., Giudici, M., 1999. Effects of sedimentary heterogeneity on groundwater flow in a quaternary pro-glacial delta environment: joining facies analysis and numerical modeling. Sedimentary Geology 129, 327–344.

Bierkens, M.F.P., 1996. Modeling hydraulic conductivity of a complex confining layer at various spatial scales. Water Resources Research 32 (8), 2369–2382.

Bierkens, M.F.P., Weerts, H.J.T., 1994. Block hydraulic conductivity of cross-bedded fluvial sediments. Water Resources Research 30, 2665–2678.

Butler, J.J., Healey, J.M., 1998. Relationship between pumping-test and slug-test parameters; scale effect or artifact? Ground Water 36 (2), 305–313.

Dagan, G., 1989. Flow and Transport in Porous Formations. Springer-Verlag.

Dagan, G., 1993. High order correction of effective permeability of heterogeneous isotropic formations of lognormal conductivity distribution. Transport in Porous Media 12, 279–290.

Danquigny, C., Ackerer, P., Carlier, J.P., 2004. Laboratory tracer tests on three-dimensional reconstructed heterogeneous porous media. Journal of Hydrology 294, 196–212.

Doll, P., Schneider, W., 1995. Lab and field measurements of the hydraulic conductivity of clayey silts. Ground Water 33 (6).

Durlofsky, L.J., 1991. Numerical calculation of equivalent grid block permeability tensors for heterogeneous porous media. Water Resources Research 27 (5), 699–708.

Dykaar, B., Kitanidis, P.K., 1992. Determination of the effective hydraulic conductivity for heterogeneous porous media using a numerical spectral approach. 2. Results. Water Resources Research 28 (4), 1167–1178.

Eggleston, J., Rojstaczer, S., 1998. Identification of large-scale hydraulic conductivity trends and the influence of trends on contaminant transport. Water Resources Research 34 (9), 2155–2168.

Fernandez-Garcia, D., Rajaram, H., Illangasekare, T.H., 2005. Assessment of the predictive capabilities of stochastic theories in a three-dimensional laboratory test aquifer: effective hydraulic conductivity and temporal moments of breakthrough curves. Water Resources Research 41, W04002. doi:10.1029/2004WR00352.

Fogg, G.E., 1990. Architecture and interconnectedness of geologic media: role of the low-permeability facies in flow and transport. Verlag Heinz Heise, Hannover, Germany, pp. 19–40.

Fogg, G.E., Carle, S.F., Green, C., 2000. Connected-network paradigm for the alluvial aquifer system. Geological Society of America Special Paper 348, 25–42.

Gelhar, L., 1993. Stochastic Subsurface Hydrology. Prentice Hall.

Gelhar, L., Axness, C., 1983. Three-dimensional stochastic analysis of macrodispersion in aquifers. Water Resources Research 19, 161–180.

Hess, K.M., Wolf, S.H., Celia, M.A., 1992. Large-scale natural gradient test in sand and gravel, Cape Cod, Massachusetts. 3. Hydraulic conductivity variability and calculated macrodispersivity. Water Resources Research 28, 2011–2027.

Hoeksema, R.J., Kitanidis, P.K., 1985. Analysis of the spatial structure of properties of selected aquifers. Water Resources Research 21, 563–572.

Hyun, Y., Neuman, S., Vesselinov, V.V., Illman, W.A., Tartakovsky, D.M., Di Federico, V., 2002. Theoretical interpretation of a pronounced permeability scale effect in unsaturated fractured tuff. Water Resources Research 38 (6), 1092. doi:10.1029/2001WR000658, 200.

Indelman, P., Abramovich, B., 1994. A higher-order approximation to effective conductivity in media of anisotropic random structure. Water Resources Research 30 (6), 1857–1864.

Jankovic, J., Fiori, A., Dagan, G., 2003. Effective conductivity of an isotropic heterogeneous medium of lognormal conductivity distribution. Multiscale Modeling and Simulation 1 (1), 40–56.

Jussel, P., Stauffer, F., Dracos, T., 1994a. Transport modeling in heterogeneous aquifers: 1. Statistical description and numerical generation of gravel deposits. Water Resources Research 30 (6), 1803–1818.

Jussel, P., Stauffer, F., Dracos, T., 1994b. Transport modeling in heterogeneous aquifers: 2. Three-dimensional transport model

and stochastic numerical tracer experiments. Water Resource Research 30 (6), 1819–1832.
Lu, S., Molz, F., Fogg, G., Castle, J.W., 2002. Combining stochastic facies and fractal models for representing natural heterogeneity. Hydrogeology Journal 10, 475–482.
Martinez-Landa, L., Carrera, J., 2005. An analysis of hydraulic conductivity scale effects in granite (full-scale engineered barrier experiment (FEBEX), Grimsel, Switzerland). Water Resources Research 4, 1W03006. doi:10.1029/2004WRR00345.
Matheron, G., 1967. Elements pour une theorie des milieux poreux. Maisson et Cie.
Matheron, G., de Marsily, G., 1980. Is transport in porous media always diffusive? A counter example. Water Resources Research 16, 901–917.
Naff, R.L., Haley, D.F., Sudicky, E.A., 1998. High-resolution Monte Carlo simulation of flow and conservative transport in heterogeneous porous media. 1. Methodology and flow results. Water Resources Research 34 (4), 663–678.
Neuman, S., 1990. Universal scaling of hydraulic conductivities and dispersivities in geologic media. Water Resources Research 26 (8), 1749–1758.
Neuman, S., 1994. Generalized scaling of permeabilities; validation and effect of support scale. Geophysical Research Letters 21 (5), 349–352.
Neuman, S.P., Di Federico, V., 2003. Multifaceted nature of hydrogeologic scaling and its interpretation. Reviews of Geophysics 41 (3). doi:10.1029/2003RG00013.
Paleologos, E.K., Sarris, T.S., Desbarats, A., 2000. Numerical estimation of effective hydraulic conductivity in leaky heterogeneous aquitards. Geological Society of America Special Paper 348, 119–127.
Paola, C., 2000. Quantitative models of sedimentary basin filling. Sedimentology 47, 121–178.
Pickup, G., Hern, C., 2002. The development of appropriate upscaling procedures. Transport in Porous Media 46, 119–138.
Renard, P., de Marsily, G., 1997. Calculating equivalent permeability: a review. Advances in Water Resources 20, 253–278.
Ronayne, M.J., Gorelick, S.M., 2006. Effective permeability of porous media containing branching channel networks. Physical Review E 73 (026305).
Rovey, C.W., 1998. Digital simulation of the scale effect in hydraulic conductivity. Hydrogeology Journal 6 (2), 216–225.
Sanchez-Vila, X., Girardi, J., Carrera, J., 1995. A synthesis of approaches to upscaling of hydraulic conductivities. Water Resources Research 31 (4), 867–882.
Sanchez-Vila, X., Carrera, J., Girardi, J., 1996. Scale effects in transmissivity. Journal of Hydrology 183, 1–22.
Scheibe, T.D., Freyberg, D.L., 1995. Use of sedimentological information for geometric simulation of natural porous media structure. Water Resources Research 31 (12), 3259–3270.
Scheibe, D., Yabusaki, S., 1998. Scaling of flow and transport behavior in heterogeneous groundwater systems. Advances in Water Resources 22 (3), 223–238.
Schulze-Makuch, D., Cherkauer, D.S., 1998. Variations in hydraulic conductivity with scale of measurement during aquifer tests in heterogeneous, porous carbonate rocks. Hydrogeology Journal 6 (2), 204–215.
Schulze-Makuch, D., Carlson, D., Cherkauer, D., Malik, P., 1999. Scale dependency of hydraulic conductivity in heterogeneous media. Groundwater 37 (6), 904–919.
Sudicky, E., 1986. A natural gradient experiment on solute transport in a sand aquifer: spatial variability of hydraulic conductivity and its role in the dispersion process. Water Resources Research 22 (13), 2069–2082.
Webb, E.K., Anderson, M.P., 1996. Simulation of preferential flow in three-dimensional, heterogeneous conductivity fields with realistic internal architecture. Water Resources Research 32 (3), 533–545.
Webb, E.K., Davis, J.M., 1998. Simulation of the Spatial Heterogeneity of Geologic Properties, an Overview. SEPM (Society for Sedimentary Geology), Tulsa, OK, United States, pp. 1–24.
Weissmann, G.S., Zhang, Y., LaBolle, E.M., Fogg, G.E., 2002. Dispersion of groundwater age in an alluvial aquifer system. Water Resources Research 38. doi:10.1029/2001WR00090.
Zhang, D., 2002. Stochastic Methods for Flow in Porous Media, Coping with Uncertainties. Academic Press.
Zhang, Y., 2005. Determination of effective hydrological parameters using experimental stratigraphy. Ph.D. Thesis, Indiana University.
Zhang, Y., Person, M., Paola, C., Gable, C., Wen, X.-H., Davis, J., 2005. Geostatistical analysis of an experimental stratigraphy. Water Resources Research 41, W11416. doi:10.1029/2004WR00375.
Zhang, Y., Gable, C.W., Person, M., 2006. Equivalent hydraulic conductivity of an experimental stratigraphy – implications for basin-scale flow simulations. Water Resources Research 42, W05404. doi:10.1029/2005WR00472.
Zhou, Q., Liu, H., Bodvarsson, G.S., Oldenburg, C.M., 2003. Flow and transport in unsaturated fractured rock: effects of multiscale heterogeneity of hydrogeologic properties. Journal of Contaminant Hydrology 60, 1–30.
Zlotnik, V.A., Zurbuchen, B.R., Ptak, T., Teutsch, G., 2000. Support volume and scale effect in hydraulic conductivity: experimental aspects. Geological Society of American Special Paper 348, 215–231.